

(*d,t*) Reactions on Nuclei with $A \approx 60$ *B. ZEIDMAN, J. L. YNTEMA, AND B. J. RAZ†
Argonne National Laboratory, Lemont, Illinois

(Received May 9, 1960)

Energy spectra of tritons from the (*d,t*) reactions on a number of nuclei with masses between $A = 51$ and $A = 68$ have been obtained at a deuteron energy of 21.5 Mev. The experiment was performed in the 60-in. scattering chamber, a double NaI crystal system being used for particle identification. The absolute differential cross sections were obtained at 27° (lab) and angular distributions of various triton groups were taken over a range of angles from 7° to 70° . The angular distributions exhibit an oscillatory behavior and have been fitted with the Butler theory for neutron pickup. The angular distributions observed in the (*d,t*) reactions on V^{51} and Cr^{52} correspond to $l=3$ transitions, while in the case of the other nuclei studied (Mn^{55} , Fe^{56} , Fe^{57} , Co^{59} , Cu^{63} , Cu^{65} , Zn^{64} , Zn^{66} , Zn^{67} , and Zn^{68}) both $l=1$ and $l=3$ transitions have been observed. Evidence for the mixing of shell-model configurations is presented. The Butler formalism and empirically determined constants have been used to extract reduced widths.

INTRODUCTION

THE use of the (*d,t*) reaction in detailed studies of nuclear reactions has previously been confined to targets with atomic weights less than 30.¹ Some survey work in other regions of the period table has also been reported.² The analysis of the (*d,t*) experiments on light targets has involved the use of the Butler theory of direct interactions.³ It has been seen that the application of the Butler theory in this region is justified since the agreement with the data is satisfactory and the conclusions drawn from the analysis are consistent with information obtained by other experimental techniques.⁴

The (*d,t*) pickup reaction provides a convenient and direct way of studying the neutron configurations of the target nuclei and, in some cases, the configuration of the states of the residual nuclei. The neutron configurations of nuclei whose mass numbers range from 50 to 70 are of interest because these configurations arise predominantly from filling of the $1f$ and $2p$ neutron shells. The study of gross structure in (*d,p*) reactions by Schiffer, Lee, and Zeidman⁵ indicated that the $1f$ and $2p$ shells do not fill sequentially and there is competition between the various configurations involving $1f$ and $2p$ neutrons. The present work contains the information obtained from the experimental study of the (*d,t*) reactions, while

the following paper⁶ will discuss the detailed interpretation of the experimental results.

The identification of the l value of picked up neutrons is made with the use of the Butler theory of direct interactions. The shape of the angular distribution of a triton group resulting from a single value of orbital angular momentum transfer l is given by the function G_l^2 , which is defined by

$$G_l^2 = \left| \frac{1}{Q^2 + k^2} [j_l(QR) - \gamma_l Q j_{l+1}(QR)] \right|^2, \quad (1)$$

where $Q = K_t - [A/(A+1)]K_d$, k is a constant determined by the binding energy of the picked up neutron, R is the interaction radius, and $j_l(QR)$ is the spherical Bessel function of order $l + \frac{1}{2}$. K_t and K_d are the wave numbers in the center-of-mass system of the triton and deuteron, respectively. Angular distributions that are fitted by $l=1$ Butler curves correspond to pickup of p neutrons, while angular distributions which are fitted by $l=3$ Butler curves correspond to pickup of f neutrons. In the course of this study, all angular distributions could be fitted by either $l=1$, or $l=3$, or a combination of $l=1$ and $l=3$. For the range of Q values involved, at an energy of 21.6 Mev, determinations of l values in (*d,t*) reactions are unique.

EXPERIMENTAL TECHNIQUES

The experiment was performed in the 60-in. scattering chamber⁷ by use of the 21.6-Mev external beam of the Argonne 60-in. cyclotron.⁸ The detection system was similar to that described previously,⁷ the detector consisting of a double NaI(Tl) crystal. The particles incident upon the detector pass through a thin (0.012 in.) dE/dx crystal and were stopped in the thick (0.160 in.) E crystal. Optical contact between the dE/dx crystal and its photomultiplier tube was made via an air light-

* Work performed under the auspices of the U. S. Atomic Energy Commission.

† Permanent Address: State University, College on Long Island, Oyster Bay, New York.

¹ M. H. Macfarlane and J. B. French, *Revs. Modern Phys.* **32**, 567 (1960). This article contains references to all (*d,t*) studies prior to 1960. N. A. Vlasov, S. P. Kalinin, A. A. Ogloblin, and V. I. Chuev, *J. Exptl. Theoret. Phys. (U.S.S.R.)* **37**, 1187 (1959) [translation: *Soviet Phys.—JETP* **10**, 844 (1960)].

² B. L. Cohen and R. E. Price, *Phys. Rev.* (to be published); N. A. Vlasov, S. P. Kalinin, A. A. Ogloblin, and V. I. Chuev, *J. Exptl. Theoret. Phys. (U.S.S.R.)* **38**, 280 (1960) [translation: *Soviet Phys.—JETP* **11**, 203 (1960)].

³ S. T. Butler, *Proc. Roy. Soc. (London)* **A208**, 559 (1951); S. T. Butler, *Nuclear Stripping Reactions* (John Wiley & Sons, Inc., New York, 1957).

⁴ A. I. Hamburger, *Phys. Rev.* **118**, 1271 (1960).

⁵ J. P. Schiffer, L. L. Lee, and B. Zeidman, *Phys. Rev.* **115**, 427 (1959).

⁶ B. J. Raz, B. Zeidman, and J. L. Yntema, following article [*Phys. Rev.* **120**, 1730 (1960)].

⁷ J. L. Yntema, Argonne National Laboratory Report ANL-5890 (unpublished); J. L. Yntema, *Phys. Rev.* **113**, 261 (1959).

⁸ W. Ramler and G. Parker, Argonne National Laboratory Report ANL-5907 (unpublished).

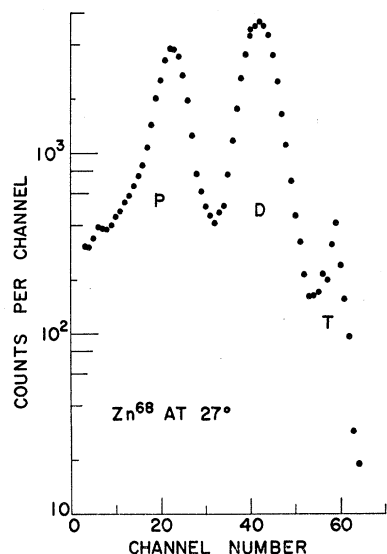


FIG. 1. The pulse-multiplier spectrum of Zn^{68} at 27° . The peaks corresponding to protons, deuterons, and tritons are labeled p , d , and t , respectively.

pipe. The signals from the E and dE/dx detectors are multiplied so that the multiplier output is proportional to MZ^2 . A multiplier output spectrum is shown in Fig. 1. The peaks correspond to protons, deuterons, and tritons and are labeled p , d , and t , respectively. The output of the multiplier was sent into a single-channel analyzer which gated a multichannel analyzer to accept the E pulses corresponding to the tritons.

Targets

The targets used were thin metallic foils which were punched from metal rolled to a thickness of approximately 0.0003 in. and weighed on a microbalance. The foils were mounted in holders and attached to the target changer which can accommodate 8 targets. Since one isotope predominates in natural V, Cr, and Fe and Mn and Co are monoisotopic, the targets of V^{51} , Cr^{52} , Mn^{55} , Fe^{56} , and Co^{59} were prepared from high-purity metal of natural isotopic abundance. The remainder of the targets were prepared from metal which had been enriched in the desired isotope by the Stable Isotope Division of ORNL.⁹

Energy Calibration

In order to identify states of the residual nuclei, it was necessary to determine the response of the E crystal as a function of the energy of the incident tritons. The effective thickness of the material between the target and the E crystal was measured by inserting absorber between the target and the detector¹⁰ until the elastically scattered deuterons failed to strike the E crystal. The effective absorber between the target and the E crystal was determined from the range-energy curves of Al and a curve of pulse height vs incident triton energy was

⁹ The foils were rolled by Mr. F. Karasek, Metallurgy Division, Argonne National Laboratory.

¹⁰ W. J. O'Neill, H. W. Ostrander, and E. G. Sundahl, Nuclear Instr. 4, 50 (1959).

calculated. Several of the reactions studied result in well isolated levels of known Q values, which serve to check the accuracy of the calibration. The calibration is good to within approximately 60 keV, which corresponds to one-half channel.

RESULTS

Energy spectra were obtained for all targets at 3° intervals between 12° and 30° and at 4° or 5° intervals from 30° to 70° . Fe^{56} was investigated over the angular range between 7° and 70° . Angular distributions have been obtained for the group structure in the various spectra, except when the spacing of levels permitted reliable separation of the contributions from individual states.

Absolute differential cross sections for the (d,t) reaction on all targets have been measured at an angle of 27° in the laboratory system. The major difficulty in measuring absolute (d,t) cross sections arises from incomplete separation of deuterons and tritons, as can be seen in Fig. 1. The majority of deuteron pulses, however, correspond to elastically scattered deuterons which have pulse heights larger than those of the most energetic tritons. The deuteron contamination of the triton spectra is, therefore, almost negligible. In order to determine the cross sections accurately, the following procedure was used. The discriminator on the particle selection system was set to accept all tritons and a considerable number of deuterons. A number of runs, characterized by successively lower ratios of deuterons to tritons, were made until no deuterons were accepted. From these runs, spectra were obtained which contained all of the tritons and had been corrected for deuteron contamination resulting from the imperfect separation of the particles. The other primary source of possible error in absolute cross section results from uncertainty in target thickness. Since the beam spot is small compared to the diameter of the foil, nonuniformities in target thickness over the face of the foil may result in variations of effective thickness. Uncertainties in the absolute cross section resulting from current integration and solid angle determination are negligible.^{7,8} The combination of these factors results in an uncertainty

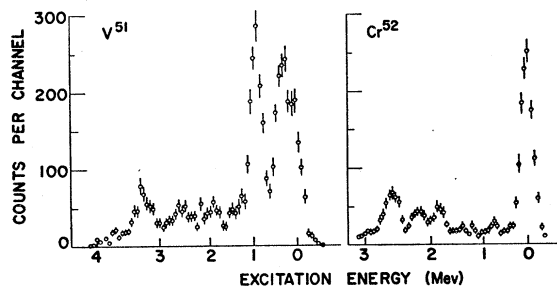


FIG. 2. Triton spectra from (a) $V^{51}(d,t)V^{50}$ and (b) $Cr^{52}(d,t)Cr^{51}$ at 27° (lab). The abscissae are the excitation energies of the residual nuclei. The ground-state Q values for the reactions $V^{51}(d,t)V^{50}$ and $Cr^{52}(d,t)Cr^{51}$ are -4.78 MeV and -5.79 MeV, respectively.

in absolute cross section at 27° which is estimated to be less than 10%. Differential cross sections at other angles were obtained relative to those at 27°.

Spectra from the various targets are shown in Figs. 2, 3, 4, and 5. It is seen that a definite pattern appears in all spectra. For targets with even neutron numbers, the reaction proceeds primarily to final states near the ground state of the residual nucleus, while the odd-neutron targets, Fe⁵⁷ and Zn⁶⁷, show relatively small cross sections to states near the ground state of the final nucleus. For the targets with odd neutron number, the reaction proceeds primarily via reactions whose Q values are similar to those of the nearby target nuclides with even neutron number.

The angular distributions of tritons leading to the ground states of the residual nuclei in the reactions Cr⁵²(d,t)Cr⁵¹ and Fe⁵⁶(d,t)Fe⁵⁵ are shown in Fig. 6. These angular distributions illustrate the two characteristic shapes of angular distributions observed in the present experiment. The Cr angular distribution exhibits an oscillatory behavior with its primary maximum at approximately 21° in the center-of-mass system and two secondary maxima. The data have been fitted with a Butler curve corresponding to neutron pickup with l=3 and a radius of 7.1 f. It would be possible to get somewhat better agreement with the primary maximum by using a radius of 6.8 f. However, there is no possibility of getting equally satisfactory agreement with the data for any other l value regardless of choice of radius.

The ground-state angular distribution for Fe⁵⁶(d,t)Fe⁵⁵ exhibits an oscillatory behavior, with the primary maximum at approximately 9° and three secondary maxima. The data is well fitted by the Butler curve for neutron pickup with l=1 and a radius of 7.4 f. Only minor variations in the radius are possible without destroying the agreement with the data. The choice of l is unique. It is to be noted that the primary maximum occurs at an angle slightly smaller than the lower limit of the angular range investigated for targets other than Fe⁵⁶.

Over the range of elements covered, it is found that

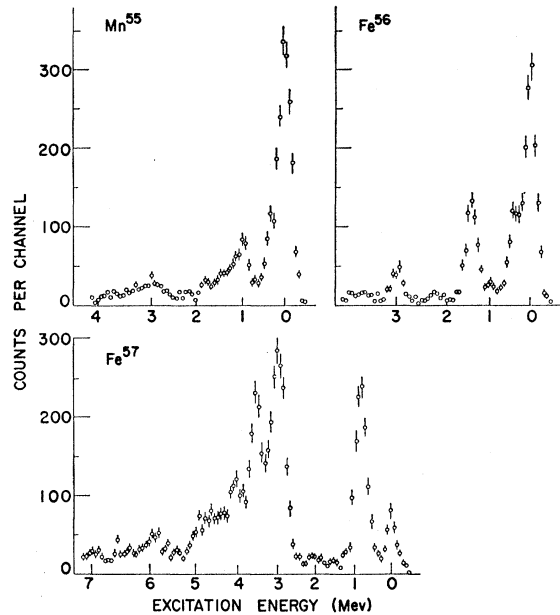


FIG. 3. Triton spectra from (a) Mn⁵⁵(d,t)Mn⁵⁴, (b) Fe⁵⁶(d,t)Fe⁵⁵, and (c) Fe⁵⁷(d,t)Fe⁵⁶ at 27° (lab). The abscissae correspond to the excitation energies of the final nuclei. The ground-state Q values are (a) -3.95 Mev, (b) -4.49 Mev, and (c) -1.37 Mev.

the angular distributions for l=1 are consistently fitted by the Butler curves for a radius of 7.4 f, and that l=3 angular distributions are consistently fitted with Butler curves for a radius of 7.1 f. Improvements in agreement may be attained for radii which differ slightly from the values given, but in all cases the agreement is quite satisfactory. In a number of cases, there is a mixture of l=1 and l=3 present in the angular distributions. For targets whose spins are zero, this arises from the failure to separate the levels in the group structure, so that the data include contributions from levels of different spins. For targets with nonzero spin, conservation of angular momentum may allow more than one value of l to be involved in the formation of a single state so that an admixture is present. For equal contributions of l=1

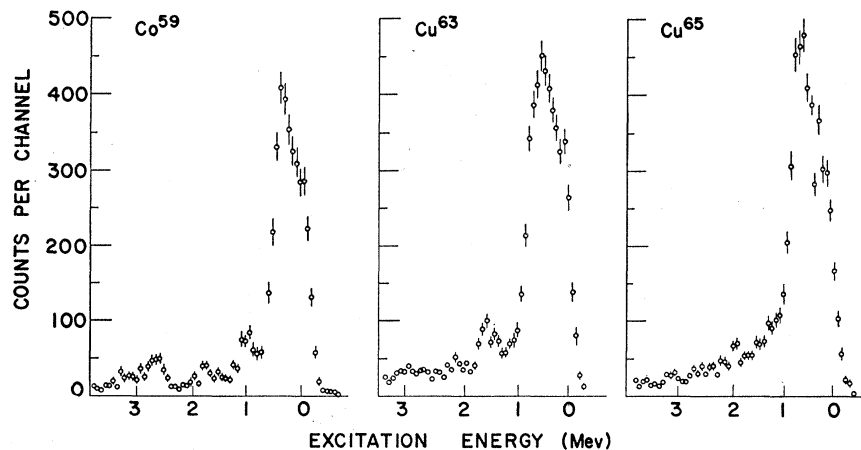


FIG. 4. Triton spectra from (a) Co⁵⁹(d,t)Co⁵⁸, (b) Cu⁶³(d,t)Cu⁶², and (c) Cu⁶⁵(d,t)Cu⁶⁴ at 27° (lab). The abscissae correspond to excitation energies of the residual nuclei. The ground-state Q values are (a) -4.24 Mev, (b) -4.54 Mev, and (c) -3.65 Mev.

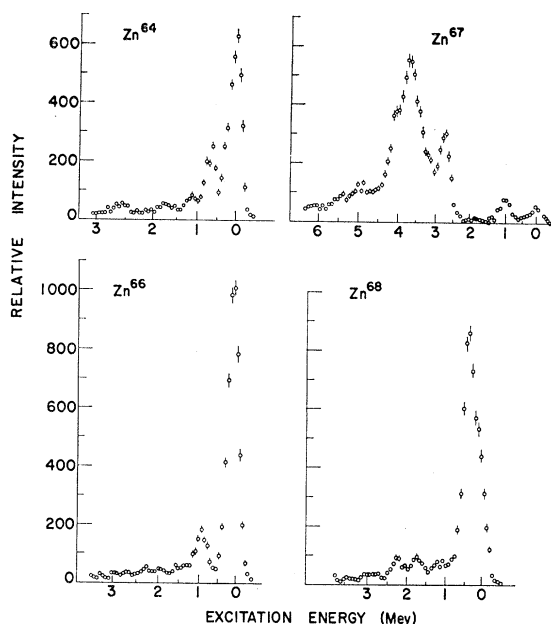


FIG. 5. Triton spectra from (a) $Zn^{64}(d,t)Zn^{63}$, (b) $Zn^{66}(d,t)Zn^{65}$, (c) $Zn^{67}(d,t)Zn^{66}$, and (d) $Zn^{68}(d,t)Zn^{67}$ at 27° (lab). The abscissae are the excitation energies of the final nuclei. The ground-state Q values are (a) -5.59 Mev, (b) -4.77 Mev, (c) -0.80 Mev, and (d) -3.93 Mev.

and $l=3$, the angular distribution will resemble an $l=1$ distribution and the resemblance to $l=1$ will become stronger as the ratio of $l=1$ to $l=3$ increases. Only if the $l=3$ is stronger than the $l=1$ will the angular distribution show an unmistakable $l=3$ shape and even then weak $l=1$ admixtures will be seen in the form of an increase in intensity at the most forward angles.

$V^{51}(d,t)V^{50}$ and $Cr^{52}(d,t)Cr^{51}$

The spectrum of the $V^{51}(d,t)V^{50}$ reaction, shown in Fig. 2, displays prominent peaks at excitation energies of 0, 0.3, 0.95, and 3.3 Mev. Other, weaker peaks are seen near 1.5, 1.9, 2.2, 2.6, and 3.1 Mev. In particular, the peak near 3.1-Mev excitation becomes quite strong at 18° and is then comparable in intensity to those at 0.3 and 0.95 Mev.

In addition to the ground-state peak, a number of much weaker groups are also observed in the spectrum of the $Cr^{52}(d,t)Cr^{51}$ reaction. There are known states in Cr^{51} at excitation energies of 0.750, 1.17, 1.42, and 1.53 Mev.¹¹ Of these, the 0.750-Mev state is seen, but weakly, and there is evidence for the 1.17-Mev state. There are definite peaks at 1.85, 2.20, and 2.60 Mev. In the region around 1.5-Mev excitation, there are a number of counts, but no structure is observed. Compared to the results on other even- N nuclei, the intensity of the 2.6-Mev group is exceptionally strong. A check of Q values

¹¹ *Nuclear Level Schemes, A=40—A=92*, compiled by K. Way, R. W. King, C. L. McGinnis, and R. van Lieshout, Atomic Energy Commission Report TID-5300 (U. S. Government Printing Office, Washington, D. C., 1955).

for the other Cr isotopes¹² does not yield a Q value for a ground-state transition or a low-lying state which would correspond to a triton of this energy.

For targets of V^{51} and Cr^{52} , each nuclide containing 28 neutrons, only $l=3$ transitions have been observed. Angular distributions have been obtained for groups leading to states near the ground state, 1.0 Mev, and 3.2 Mev in V^{50} and to the ground state and 0.75 Mev in Cr^{51} . Since no $l=1$ transitions are observed, there appears to be little or no configuration mixing with the $p_{3/2}$ shell which lies above the $f_{7/2}$ shell in the single-particle shell model.

$Mn^{55}(d,t)Mn^{54}$

Figure 3 shows the spectrum obtained at 27° for Mn^{55} . Peaks corresponding to excitation energies of 0, 0.40, 0.70, 1.00, 1.40, 1.80, and 2.2 Mev in Mn^{54} were observed. There is evidence for other groups at approximately 2.7-, 3.0-, 3.3-, 3.7-, 3.9-, and 4.5-Mev excitation. The peaks corresponding to the ground state and 1-Mev level predominate. Previous data from the $Fe^{57}(p,\alpha)Mn^{54}$ reaction¹³ indicated states at 0, 0.160, and 0.410 Mev. There was no possibility of resolving the 0.160-Mev level, if present, in our case.

Angular distributions of groups leading to states near 0, 1.0, 2.7, and 4.0 Mev in Mn^{54} have been obtained. The ground state, 2.7 Mev, and 4.0-Mev groups are characterized by $l=1$ angular distributions. The 1.0-Mev state is primarily an $l=3$ angular distribution with about a 10% admixture of $l=1$.

$Fe^{56}(d,t)Fe^{55}$

The states of Fe^{55} have been carefully investigated previously and 138 levels have been observed up to an excitation of 7.5 Mev.¹⁴ In the $Fe^{56}(d,t)Fe^{55}$ reaction,

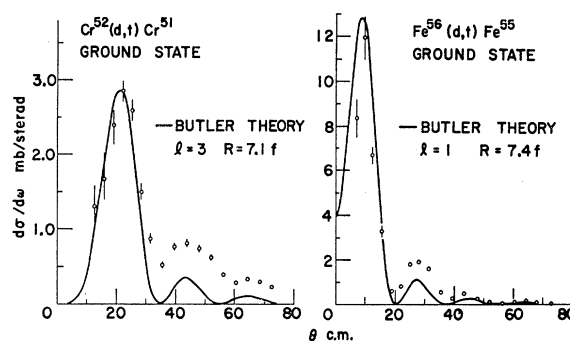


FIG. 6. Angular distributions of the ground-state reactions in (a) $Cr^{52}(d,t)Cr^{51}$ and (b) $Fe^{56}(d,t)Fe^{55}$. The solid curves are computed from the Butler theory for (a) $l=3$, $R=7.1$ f and (b) $l=1$, $R=7.4$ f.

¹² V. J. Ashby and H. C. Catron, University of California Radiation Laboratory Report, UCRL-5419 (unpublished).

¹³ A. Sperduto, Massachusetts Institute of Technology Laboratory for Nuclear Science Progress Report AECU-3908 May, 1958 (unpublished).

¹⁴ K. Way *et al.* *Nuclear Data Sheets* (National Academy of Sciences-National Research Council). This continuing compilation of data contains all pertinent references.

the levels at 0, 0.413, and 0.933 Mev have been resolved. There is a strong peak at 1.4 Mev which could include the 1.322-, 1.413-, and 1.504-Mev levels. From the position and shape of the peak, it is concluded that the 1.413-Mev level is dominant. Other groups are seen at 2.05-, 2.3-, 2.9-, 3.1-, 3.4-, 3.7-, and 4.0-Mev excitation. The states at 0 and 0.415 Mev and the groups at 1.4, 1.9, and 2.5 Mev have been analyzed. The ground state, 0.415-Mev level, and 1.9-Mev group have $l=1$ angular distributions, while the 2.5-Mev group has an $l=3$ angular distribution. The group at 1.4 Mev is primarily an $l=3$ with about a 15% admixture of $l=1$. The beta decay of Co^{55} , which is presumed to have a spin and parity of $\frac{7}{2}^-$, proceeds primarily to the 1.413- and 0.933-Mev states of Fe^{55} with $\log ft$ values of 5.7 and 6.4, respectively.¹³ These $\log ft$ values are within the range of allowed transitions so that the assumption of $\frac{7}{2}^-$ spin and parity for Co^{55} would set limits of $\frac{5}{2}^-$ to $9/2^-$ for the spins and parities of the 1.413- and 0.933-Mev levels of Fe^{55} . The present results indicate that the 1.413-Mev state is dominant in the 1.4-Mev group. The angular distribution of the group then sets a limit of $\frac{7}{2}^-$ or $\frac{5}{2}^-$ for this state. The lack of transitions to the ground state and the 0.415-Mev state in Co^{55} beta decay is also consistent with the spins and parities of either $\frac{3}{2}^-$ or $\frac{1}{2}^-$ obtained from the present work.

$\text{Fe}^{57}(d,t)\text{Fe}^{56}$

The $\text{Fe}^{57}(d,t)\text{Fe}^{56}$ spectrum shown in Fig. 3 exhibits a number of prominent peaks which can be compared to the known levels in Fe^{56} . The levels at 0 and 0.845 Mev have been resolved, as is the $\text{Fe}^{56}(d,t)\text{Fe}^{55}$ ground-state transition which corresponds to an excitation of 3.57 Mev in Fe^{56} . There is some evidence for the presence of the 2.085-Mev state of Fe^{56} , but the intensity of this peak is too weak to permit definite identification. The very strong peak at 2.95-Mev excitation may be due to the excitation of the 2.940- and 2.958-Mev levels. Other groups are observed at 4.0-, 4.3-, 5.0-, 5.4-, 5.6-, 5.85-, and 6.4-Mev excitation. Since the Fe^{57} target contained 23% Fe^{56} , levels between 3.3- and 3.8-Mev excitation are obscured by the $\text{Fe}^{56}(d,t)\text{Fe}^{55}$ ground-state transition. The contribution of the Fe^{56} has been subtracted in making level assignments.

Angular distributions of tritons leading to the ground state and 0.845-Mev state of Fe^{56} from the reaction $\text{Fe}^{57}(d,t)\text{Fe}^{56}$ are shown in Fig. 7. The ground-state transition is a pure $l=1$, in excellent agreement with the Butler curve. The spin and parity of Fe^{57} is known to be $\frac{1}{2}^-$. Since Fe^{56} has a spin and parity of 0^+ , the ground-state transition must involve pickup of a $p_{\frac{1}{2}}$ neutron. The presence of this term in the wave function of Fe^{57} is definite evidence for the mixing of shell-model configurations. Since the spin and parity of the 0.845-Mev state of Fe^{56} is 2^+ , both $l=1$ and $l=3$ transitions to this state from the Fe^{57} ground state are allowed. The fact that the data show that both $l=3$ and $l=1$ transitions

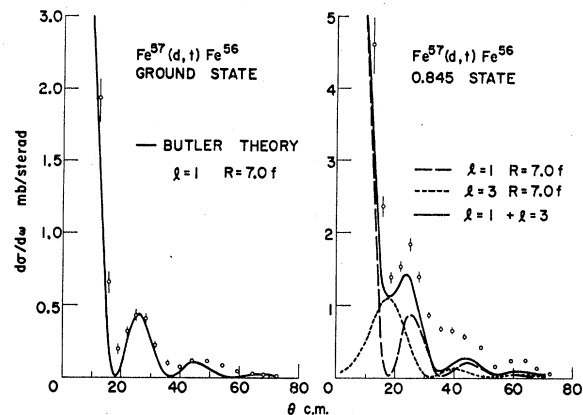


FIG. 7. Angular distributions from $\text{Fe}^{57}(d,t)\text{Fe}^{56}$. (a) Angular distribution of the ground-state triton peak. The solid curve corresponds to the Butler theory for $l=1$, $R=7.0$ f. (b) Angular distribution of tritons leading to the 0.845-Mev state in Fe^{56} . The curves correspond to the Butler theory. The long dashes are for $l=1$, $R=7.0$ f, the short dashes for $l=3$, $R=7.0$ f, and the solid curve results from the addition of the dashed curve.

do contribute, is further evidence that configuration mixing is involved. The angular distribution for the 0.845-Mev state illustrates the difficulty in separating $l=3$ admixtures from $l=1$ curves. In this case, the $l=1$ and $l=3$ intensities are roughly equal, yet the angular distribution appears primarily as an $l=1$. The angular distribution of the 2.95-Mev group appears to be a pure $l=1$ transition. This is consistent with the assignment of the spin and parity of 2^+ for the 2.958-Mev state, which has been made on the basis of the beta decay of Mn^{56} and the angular correlation of the cascade gamma rays.¹⁴ The angular distribution of the 4-Mev group corresponds to an $l=3$ transition. The two known states in the region which contribute to this group are the 3.84-Mev (3^+ or 5^+) and 4.10-Mev (4^+) levels. If the 3.84-Mev level contributes strongly, then its spin and parity must be 3^+ , since conservation of angular momentum sets an upper limit of 4 for the spin of the final state.

$\text{Co}^{59}(d,t)\text{Co}^{58}$, $\text{Cu}^{63}(d,t)\text{Cu}^{62}$, and $\text{Cu}^{65}(d,t)\text{Cu}^{64}$

The spectra for targets of Co^{59} , Cu^{63} , and Cu^{65} are shown in Fig. 4. All three show a similar spectral shape of a wide, asymmetric peak whose mean is several hundred kilovolts above the ground state and then a much lower yield to higher excited states. In particular, the $\text{Co}^{59}(d,t)\text{Co}^{58}$ spectrum indicates a ground-state Q value which is approximately 100 keV less negative than that which has been obtained from mass values.¹² In view of the accuracy of the energy calibration as evidenced by comparison with other known Q values, it is felt that this discrepancy is significant. The peak of the broad group corresponds to 0.49-Mev excitation, relative to the calculated ground state. Other groups appear at 1.0, 1.8, 2.1, 2.7, and 3.1 Mev.

In the beta decay of Zn^{62} , states in Cu^{62} have been

observed at 0, 0.042, 0.30, 0.55, 0.63, and 0.70 Mev. These states essentially cover the region of the broad group. Other weaker groups are seen at 1.1, 1.4, 1.6, 2.15, 2.7, 2.9, and 3.9 Mev.

A number of levels in Cu^{64} have been observed in the $\text{Cu}^{63}(d,p)\text{Cu}^{64}$ reaction. With the exception of the 0- and 0.16-Mev levels, there appears to be a band structure in the level diagram for low excitations. The levels appear to cluster about 0.3, 0.65, 0.90, 1.31, and 1.50 Mev. The broad peak has a fine structure which indicates peaks at about 0.30 Mev and 0.65 Mev. There are indications for other groups in the spectrum at 1.3-, 1.5-, 2.0-, 2.2-, and 3.2-Mev excitation.

Angular distributions have been obtained for the broad groups in Co^{58} , Cu^{62} , and Cu^{64} and for the group at approximately 1.5-Mev excitation in Cu^{62} . All of these angular distributions appear to correspond to $l=1$. If, however, there are some $l=3$ contributions, as would be expected on the basis of the shell model, then such $l=3$ contributions could easily be masked if the intensity of the $l=3$ were less than the intensity of the $l=1$. Since the $l=3$ angular distributions peak at the position of the first minimum of the $l=1$ angular distribution, an upper limit for the $l=3$ contributions can be obtained.

$\text{Zn}^{64}(d,t)\text{Zn}^{63}$

From the position of the ground-state peak in the $\text{Zn}^{64}(d,t)\text{Zn}^{63}$ spectrum, shown in Fig. 5, it is concluded that the peak results primarily from transitions to the ground state. The asymmetry of the peak indicates that the 0.19-Mev level is also present. There is a prominent peak corresponding to the 0.64-Mev level of Zn^{63} and definite indications of the presence of the 1.04-Mev level. Other groups appear at 1.74- and 2.55-Mev excitation.

The angular distribution of the ground-state group in the $\text{Zn}^{64}(d,t)\text{Zn}^{63}$ angular distribution corresponds to $l=1$, but there is, once again, the possibility of an $l=3$ admixture. From the peak shapes, however, it appears that the ground-state angular distribution corresponds to $l=1$, and any $l=3$ admixture in the angular distribution would result from transitions to the 0.19-Mev state of Zn^{63} . From conservation of angular momentum, the ground-state spin and parity of Zn^{63} is $\frac{1}{2}^-$ or $\frac{3}{2}^-$. From the beta decay of Zn^{63} , it is inferred that the spin and parity of Zn^{63} is $\frac{3}{2}^-$ or $\frac{5}{2}^-$. It is therefore concluded that the spin and parity of Zn^{63} is $\frac{3}{2}^-$, since this is the only value permitted by both measurements. The angular distributions of the groups at 0.64 Mev and 1.04 Mev in Zn^{63} are also fitted with $l=1$. If more detailed investigation of the level structure of Zn^{63} shows that these levels are indeed single levels, then the spins and parities of these levels are $\frac{1}{2}^-$ or $\frac{3}{2}^-$, and no admixture of $l=3$ is present. If, however, the observed 0.64- and 1.04-Mev levels are really several closely spaced levels, then an $l=3$ admixture is possible.

$\text{Zn}^{66}(d,t)\text{Zn}^{65}$

The $\text{Zn}^{66}(d,t)\text{Zn}^{65}$ spectrum is characterized by a very strong peak near the ground state, a weaker peak at 0.90-Mev excitation and only the barest indications of groups at approximately 1.4-, 1.9-, and 2.3-Mev excitation. The maximum of the ground-state peak occurs at approximately 0.10-Mev excitation, which corresponds to the position of the presumed $\frac{3}{2}^-$ state at 0.115-Mev excitation.¹³ Other known levels covered by this peak are the ground state and levels at 0.054- and 0.209-Mev excitation. The shape of the peak indicates that the 0.115-Mev level is responsible for most of the intensity observed. The peak at 0.90 Mev is consistent with the known level at 0.86 Mev.

The angular distribution of the ground-state group in the $\text{Zn}^{66}(d,t)\text{Zn}^{65}$ agrees with that for $l=1$ with the possibility of an $l=3$ admixture. From the beta decays of Zn^{65} and Ni^{65} to Cu^{65} , the spin and parity of Zn^{65} is presumed to be $\frac{5}{2}^-$, so the ground-state transition in the $\text{Zn}^{66}(d,t)\text{Zn}^{65}$ reaction should be characterized by an $l=3$ angular distribution. Since the most intense level in the ground-state group is the 0.115-Mev level, the angular distribution of the group is then consistent with a spin and parity of $\frac{3}{2}^-$ for the 0.115-Mev level. The angular distribution of the 0.90-Mev group is fitted by $l=1$, which then sets limits of $\frac{1}{2}^-$ or $\frac{3}{2}^-$ for the spin and parity of this state. If the ground-state spin and parity is indeed $\frac{5}{2}^-$ and that of the 0.115-Mev state $\frac{3}{2}^-$, then one would expect to see gamma emission to both the ground state and the 0.115-Mev state in the decay of the 0.86-Mev level, if its spin and parity were $\frac{3}{2}^-$. Since the 0.86-Mev level is seen to decay only to the 0.115-Mev level, it is then most probable that the spin and parity of the 0.86-Mev level is $\frac{1}{2}^-$. This would then indicate that a $p_{3/2}$ admixture is present in the Zn^{66} ground-state configuration.

$\text{Zn}^{67}(d,t)\text{Zn}^{66}$

The spectrum of the $\text{Zn}^{67}(d,t)\text{Zn}^{66}$ reaction shows peaks corresponding to the known levels at 0, 1.05, 2.75, and 3.78 Mev.¹¹ There is definite evidence for the presence of the known levels at 3.24 and 4.10 Mev and some indications of the 4.3-Mev state. The transition to the 2.40-Mev state is weak, if it exists at all. The Zn^{67} target was enriched to 81% Zn^{67} , the remainder being roughly equal parts of Zn^{64} , Zn^{66} , and Zn^{68} . In the region corresponding to excitations between 4.5 and 5.0 Mev in Zn^{66} , (d,t) reactions on these last isotopes of zinc contribute, but cannot account for all of the observed intensity. After correction for the isotopic mixture, the spectra indicate substantial cross sections to levels between 4.5 and 5.0 Mev, but no group structure is seen.

Angular distributions from the $\text{Zn}^{67}(d,t)\text{Zn}^{66}$ reactions have been obtained for transitions leading to the ground, 1.05-Mev, and 2.75-Mev states and to the group at about 3.75 Mev in Zn^{66} . The ground-state transition is

fitted with an $l=3$ curve, which is consistent with the spins $\frac{5}{2}^-$ and 0^+ for the ground states of Zn^{67} and Zn^{66} , respectively. The other angular distributions are mixtures of weak $l=1$ and strong $l=3$. Since both $l=1$ and $l=3$ transitions are observed to the 1.05- and 2.75-Mev levels, the spins and parities of these states must lie between 2^+ and 4^+ . This is consistent with the spin of the 1.05-Mev level, which is known to be 2^+ .

$\text{Zn}^{68}(d,t)\text{Zn}^{67}$

The $\text{Zn}^{68}(d,t)\text{Zn}^{67}$ reaction yields spectra, of which one is shown in Fig. 5, characterized by a strong peak near the ground state and much weaker peaks at approximately 1.0-, 1.7-, and 2.25-Mev excitation. The peak at 1.7 Mev corresponds to a known level at this excitation. The known levels at 0.87 and 0.98 Mev may be contributing to the 1.0-Mev peak. Near the ground state, levels at 0, 0.93, 0.184, 0.388, and 0.59 Mev have been observed in the beta decays of Cu^{67} and Ga^{67} . The ground-state peak is quite broad and covers all of these levels. The peak has a maximum corresponding to approximately 0.40-Mev excitation, which is in good agreement with the 0.388-Mev level. Since the other levels are relatively well separated from this one, it is concluded that the 0.388-Mev level is strongly excited. There is a slight plateau at 0.10-Mev excitation which is in agreement with the 0.093-Mev level. At angles of 18° or 21° the shape of the peak is somewhat altered and there is definite evidence that the 0.184-Mev level and the ground state are excited. There is no indication of the presence of the 0.59-Mev state, but it may be hidden by the low-energy tail of the 0.388-Mev peak.

The angular distribution of the ground-state group is well fitted by an $l=1$ curve. The most intense part of this group results from excitation of the 0.388-Mev level, a result which is consistent with a presumed spin and parity of $\frac{3}{2}^-$ obtained from the beta decays of Ga^{67} and Cu^{67} . From the change in peak shape with angle, there are definite indications that both the ground and 0.184-Mev states have angular distributions which are in agreement with the Butler curve for an $l=3$ transition. The 0.093-Mev level appears to have an angular distribution of the same shape as the 0.388-Mev level, which is $l=1$. The l values for the individual levels are then consistent with the spins and parities obtained from the beta-decay work.

Calculations of Reduced Widths

Reduced widths have been extracted for the levels and groups for which angular distributions have been obtained. To determine absolute reduced widths, it is essential to have information concerning absolute cross sections and the angular dependence of the groups. These are then compared with the Butler theory in order to obtain the reduced widths.

The Butler form for the differential cross section for

TABLE I. Reduced widths for strong groups. The groups are listed according to excitation in the final nucleus. The absolute differential cross section for each group at approximately 28° (c.m.) is given in mb/sr. The symbols $\theta^2(1)$ and $\theta^2(3)$ designate reduced widths for $l=1$ and $l=3$, respectively. The "less than" symbol indicates an upper limit for an unobserved $l=3$ contribution.

Final nucleus	Level	$d\sigma/d\omega(28^\circ)$ mb/sr	100 $\theta^2(1)$	100 $\theta^2(3)$
$^{23}\text{V}^{50}$	0.3	1.6		1.8
	1.1	1.5		1.6
	3.1	0.7		1.3
$^{24}\text{Cr}^{51}$	0	1.5		2.9
	0.75	0.2		0.4
$^{25}\text{Mn}^{54}$	0	2.5	2.9	
	1.1	0.87	0.5	1.0
	2.7	0.41	0.5	
	4.0	0.16		0.2
$^{26}\text{Fe}^{55}$	0	2.0	1.6	
	0.42	0.65	0.4	
	1.4	1.0	0.2	1.4
	2.0	0.15	0.1	
	2.5	0.10		0.1
$^{26}\text{Fe}^{56}$	0	0.40	0.38	
	0.85	1.4	0.76	0.70
	2.9	2.0	1.82	
	4.0	0.70		0.93
$^{27}\text{Co}^{58}$	0.3	5.3	5.3	<2.2
$^{29}\text{Cu}^{62}$	0.4	4.7	3.8	<2.0
	1.4	0.68	0.7	<0.4
$^{29}\text{Cu}^{64}$	0.4	7.8	6.4	<4.0
$^{30}\text{Zn}^{63}$	0	3.3	3.3	<1.5
	0.64	0.78	0.9	<0.3
	1.1	0.37	0.4	<0.2
$^{30}\text{Zn}^{65}$	0	6.0	3.85	<2.35
	0.86	1.1	0.75	<0.5
$^{30}\text{Zn}^{66}$	0	0.25		0.29
	1.0	0.33	0.35	0.20
	2.7	1.85	0.64	0.91
	3.7	3.85	1.5	1.0
$^{30}\text{Zn}^{67}$	0.3	7.5	4.5	3.7

neutron pickup via a (d,t) reaction may be expressed as

$$\frac{d\sigma}{d\omega} = \Lambda \frac{A(A+1) K_t R}{(A+3)^2 K_d \gamma_l^2} G_l^2 \theta^2, \quad (2)$$

where Λ is a constant containing the overlap of the deuteron and triton wave functions, A is the mass of the residual nucleus, θ^2 is the reduced width for the transition, G_l^2 [given by Eq. (1)] is the term containing the angular dependence of differential cross section, and γ_l is defined as

$$\gamma_l = \frac{h_l(ikR)}{ikh_{l+1}(ikR)}, \quad (3)$$

where h_l is the spherical Hankel function of order $l+\frac{1}{2}$.

To determine the reduced width, it is desirable to determine the differential cross section at the primary peak of the angular distribution. The range covered by the angular distributions encompasses the primary peak for groups corresponding to $l=3$ transitions, but not for $l=1$ transitions. However, this range was extended in the study of the $\text{Fe}^{56}(d,t)\text{Fe}^{55}$ reaction. Since the energies of the various $l=1$ groups in other targets do not vary greatly from those in Fe^{56} , it is reasonable to

assume that the ratio of the second maximum to the primary maximum is approximately the same as in $\text{Fe}^{56}(d,t)\text{Fe}^{55}$. The shapes of the angular distributions for all $l=1$ groups, including those from the Fe^{56} target, are very similar. Estimating the intensity of the primary maximum on the basis of that of the secondary maximum is believed to introduce a possible error of no more than 10% into the resulting reduced width.

Another possible source of error in the reduced widths results from the choice of the value of Λ . The value of Λ is obtained from comparison of (d,p) , (p,d) , and (d,t) reactions which proceed between the same two levels. On the basis of data which extend up to $A=25$, Macfarlane¹ finds $\Lambda=195\pm 35$. This is the value used in the present calculations. There may be a large deviation from this value of Λ in the region of A investigated in the present work, but in the absence of any additional information no better estimate can be made. The reduced widths given in Table I may be simply corrected for any improved value of Λ by keeping the product $\Lambda\theta^2$ constant.

Apart from the errors involved in determining Λ , all possible sources of experimental error introduce less than 20% error into the reduced widths obtained here. The reduced widths for the various levels and groups are given in Table I, where $\theta^2(1)$ refers to angular distributions corresponding to $l=1$ transitions and $\theta^2(3)$ refers to angular distributions corresponding to $l=3$ angular distributions. The groups are listed according to residual nuclides and excitation energy in the nucleus. The "less than" symbol indicates the absence of an observed $l=3$ transition when one is possible, the listed value for the reduced width then being an upper limit on the $l=3$ contribution as set by the cross section at the minimum of the observed $l=1$ angular distribution.

ACKNOWLEDGMENTS

We wish to acknowledge the cooperation of W. Ramler and the cyclotron group and the assistance of W. J. O'Neill and S. Piascek in obtaining and analyzing data. We also wish to thank Dr. M. H. Macfarlane for a number of stimulating discussions and suggestions.

Analysis of the Structure of Nuclei from (d,t) Reactions*

B. J. RAZ

Argonne National Laboratory, Argonne, Illinois, and State University of New York, Oyster Bay, New York

AND

B. ZEIDMAN AND J. L. YNTEMA

Argonne National Laboratory, Argonne, Illinois

(Received May 9, 1960)

The following work illustrates the use of experimentally determined reduced widths from (d,t) reactions in analyzing the structure of the ground state of the target nuclei. The (d,t) reaction is an especially sensitive and almost unique experimental technique for measuring small components of nuclear wave functions. In this role it becomes a valuable tool in investigating the presence of strong pairing forces in nuclei. This analysis demonstrates the strong mixture of the $2p_{3/2}$ and $1f_{5/2}$ neutron states in the region around $A=60$. In contrast to this, nuclei with 28 neutrons show no observable mixing of states. Special attention is given to Fe^{57} and a shell-model wave function is derived that gives the observed magnetic moment as well as the observed (d,t) reduced widths. In this connection a simple general formula is presented for the magnetic moment of any shell-model wave function.

I. INTRODUCTION

THE Butler theory of nuclear reactions¹ has been a most productive theory in the fields of (a) the mechanism of nuclear reactions, and (b) nuclear structure and spectroscopy. In this paper the primary interest is in area *b*. The Butler theory is used as an empirical tool in analyzing (d,t) pickup experiments in order to extract information about nuclear wave functions.

* This work was performed under the auspices of the U. S. Atomic Energy Commission.

¹ S. T. Butler, Proc. Roy. Soc. (London) **A208**, 559 (1951). See also S. T. Butler, *Nuclear Stripping Reactions* (John Wiley & Sons, Inc., New York, 1957) for a complete list of references to the early work in this field.

This application of Butler theory was first used by Bethe and Butler² to estimate the l value admixtures in certain nuclear wave functions. Since that time several authors³ have extended this technique and demonstrated its usefulness in determining nuclear structure. The most recent work in this field is that of Macfarlane and French,⁴ who have made a complete

² H. A. Bethe and S. T. Butler, Phys. Rev. **85**, 1045 (1952).

³ See, for example, J. B. French and B. J. Raz, Phys. Rev. **104**, 1411 (1956); T. Auerbach and J. B. French, Phys. Rev. **98**, 1276 (1955); A. M. Lane, Proc. Phys. Soc. (London) **A66**, 977 (1953); and S. Okai and M. Sano, Progr. Theoret. Phys. (Kyoto) **14**, 399 (1955), and **15**, 203 (1956).

⁴ M. H. Macfarlane and J. B. French, Revs. Modern Phys. **32**, 567 (1960).